8.1 SINGLE COLUMN MODELING OF THE DIURNAL CYCLE BASED ON CASES99 DATA – GABLS SECOND INTERCOMPARISON PROJECT

Gunilla Svensson[1*] and Albert A. M. Holtslag[2]
[1]University of Colorado/CIRES, Boulder, CO, USA
[2]Wageningen University, Wageningen, The Netherlands

1. INTRODUCTION

The general goal of the GEWEX Atmospheric Boundary Layer Study (GABLS – GEWEX stands for the Global Energy and Water Cycle Experiment) is to improve the understanding of the atmospheric boundary layer and its representation in regional and large-scale climate models (Holtslag, 2003; 2006). The first GABLS intercomparison study focused on the model representation of stable boundary layers using a rather academic set-up and utilizing Large Eddy Simulation results as a reference for the column models (Beare et al., 2006; Cuxart et al., 2006). For the second modeling intercomparison exercise, a case based on CASES99 observations is selected (Poulos et al., 2002). The main purpose of the second study is to examine to what extent the diurnal cycle over land is well represented by the boundary layer schemes included in today's numerical weather prediction (NWP) and climate models as well as in research models.

The CASES99 data is selected because of its relative flat location, dry surroundings and clear sky conditions. The case thus well represents a textbook case of a radiation forced diurnal cycle. Note that Steeneveld et al. (2006) performed a case study with these data and found good agreement with their model set up which besides of boundary-layer turbulence allowed for surface feedback and radiation processes. In this study, we focus on the intercomparison of various boundary layer schemes and prescribe the surface temperature as inspired by the observations. In addition, we simplify the various forcing terms to facilitate a better intercomparison.

2. CASE SETUP AND PARTICIPATING MODELS

The CASES99 dataset was collected during October 1999 in Kansas, US (37.6N, 96.7W). In this study, we focus on two diurnal cycles during the period 23-24 October. When designing the model experiment, our ambition was to keep the setup of the simulation as simple as possible to make it possible for many groups to participate and to secure that model specific implementation of more complicated processes would not obscure the results. Thus, the participating single-column models (SCMs) are all driven by the prescribed surface temperature (see Fig. 1), constant geostrophic wind (see Fig. 2) and a small subsidence rate starting in the afternoon of 23 October. Details about the case setup, background figures, model details and more analysis results can be found at http://www.misu.su.se/~gunilla/gabls.

To find a situation in atmospheric observational data that is horizontal homogeneous and quasi-stationary is extremely difficult. As mentioned above, a constant geostrophic wind was used to force the SCMs. If not, oscillations are easily introduced in the model solutions due to inertia effects (e.g. Svensson and Holtslag, 2006). To examine the large-scale flow, we diagnosed the geostrophic wind from the pressure field of a three-dimensional simulation using COAMPS® (Hodur, 1997). Figure 2 shows the temporal evolution of the winds at approximately 3000 m height above the surface. The geostrophic wind is approximately constant for the first 12 hours and then there is an almost linear decrease for the next 24 hours. There is no directional change during this time frame. In the morning of the October 24, there are other significant changes in wind speed and direction as well as temperature that end the quasi-stationary conditions required for the comparison with data. The first hours of the SCMs results are omitted to allow for some model spin-up. The comparison with data is thus from 20LT October 22 – 07LT October 24, i.e. two full nights and the intermediate day.

In Table1, the participating models are presented. They represent many of the major NMW prediction center as well as a variety of research models. Both models with prognostic turbulent kinetic energy as well as first orders models are represented. Some centers have run their model either with additional closures or with higher resolutions. The color-coding of the models can be found in Figure 3, the thin lines show additional runs done with some of the models.

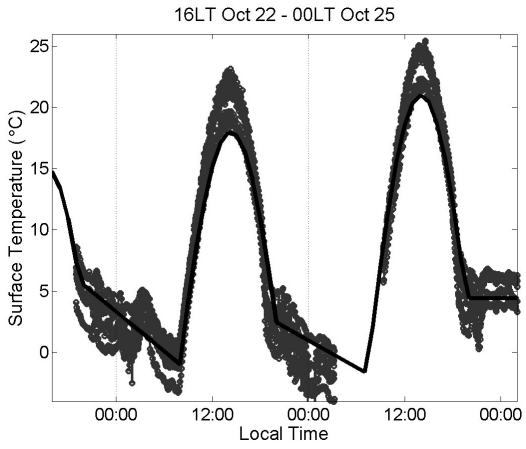

Figure1. The prescribed (solid line) and observed surface temperature (markers) around the main tower for the entire simulated period.

* Corresponding address: On leave from Department of Meteorology, Stockholm University, S-106 91 Stockholm, Sweden; e-mail: gunilla@misu.su.se

Table 1. The participating models.

MODEL	TYPE	CONTACT	AFFILIATION
ACM2	1st order	Jon Pleim	Atmospheric Science Modeling Division/NOAA NERL/USEPA
COAMPS®	TKE	Stefan Söderberg	MISU, Stockholm, Sweden
ECMWF	1st order	Anton Beljaars	ECMWF, UK
EL	E-l	Wensong Weng	York University, Canada
GSP_KI	K-l	Boris Galperin	
ISAC_Oper	1st order	Matteo Zampieri	ISAC-CNR, Bologna, Italy
ISAC_Res	E-l		
JMA_OP	1st order	Hiroto Kitagawa	Japan Meteorological Agency
JMA	1st order		
KEPS	K-e	Frank Freedman	SJSU
KNMI_635	E-l	Cisco de Bruijn	KNMI, The Netherlands
KNMI_635a			
LaRC	TKE	Anning Cheng	NASA, LaRC/Hampton University
MESONH_CNRM	TKE	Valery Masson	CNRM/GMME/TURBAU, Toulouse, France
MFOPE	1st order	Eric Bazile	CNRM/GMAP/PRO, Toulouse, France
MFOPE_HR	1st order		
MFTKE	TKE		
MFTKE_HR	TKE		
MIUU	TKE	Gunilla Svensson	MISU, Stockholm, Sweden
MO_OP	1st order	Anne Mccabe	Met Office, UK
MO_OP_70	1st order		
MO_SHARP	1st order		
MO_SHARP_70	1st order		
MSC	e-l	Jocelyn Mailhot	MSC, Dorval, QC, Canada
NCEPgfs	1st order	Frank Freedman & Michael Ek	NCEP, USA
YSU	1st order		
UIBUPC	TKE	Joan Cuxart & Laura Conangla	Universitat de les Illes Balears Universitat Politècnica de Catalunya Spain
WUR_D91	1st order	Gert-Jan Steeneveld & Bert Holtslag	Meteorology and Air Quality Section, Wageningen University, The Netherlands

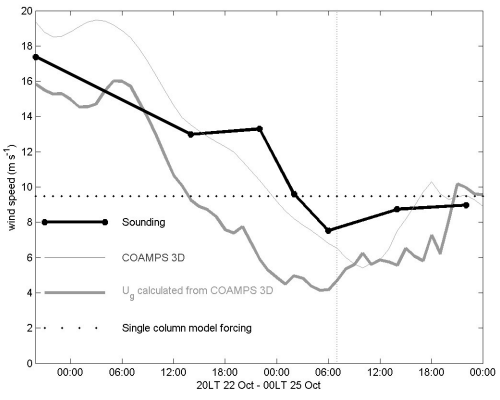

Figure 2. The geostrophic wind analyzed from the three-dimensional COAMPS® simulation (solid gray line) together with the simulated wind (thin gray line) and rawinsoundings (dark dots with linear combination). The dotted line shows the forcing for the SCMs.

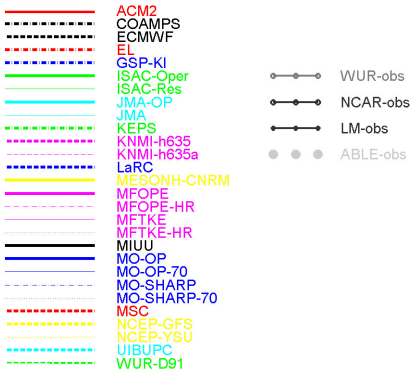

Figure 3. Legend for the models and the various observations presented in Figures 3 – 7.

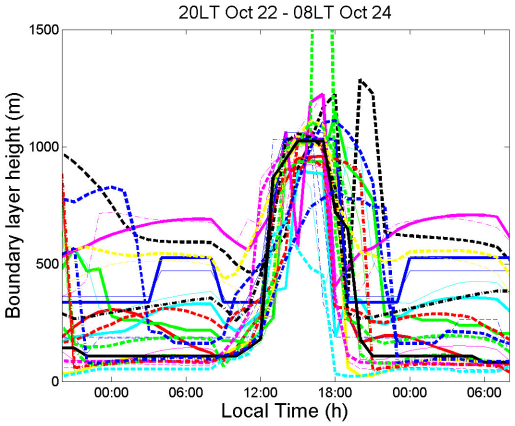

Figure 4. Boundary-layer height (m). For color-coding see Fig. 3.

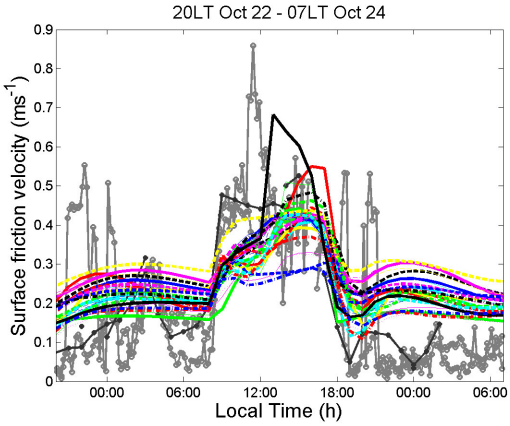

Figure 6 Surface friction velocity (ms^{-1}). For color-coding see Fig 3.

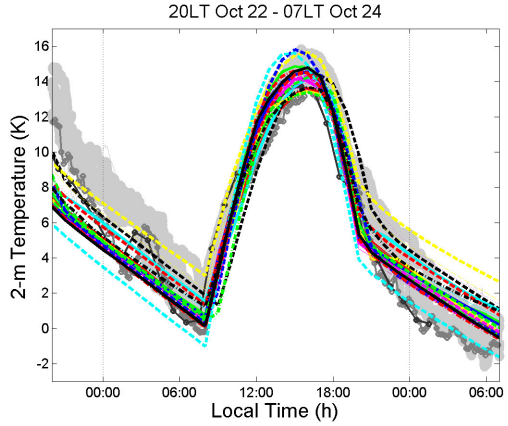

Figure 5. Surface air temperature (^{o}C) at 2 m height. For color-coding see Fig. 3. The gray lines are tower observations from the main site and the gray dots represent an area of approximately 50x50km^2 around the main tower.

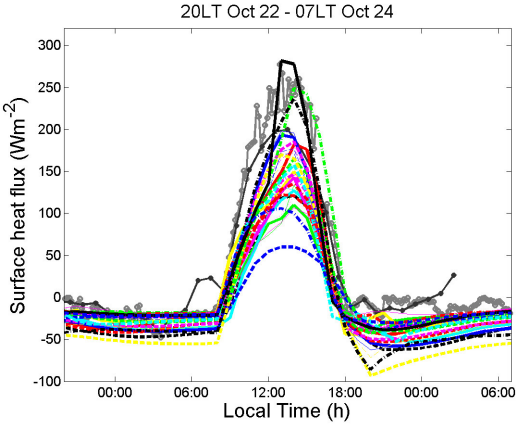

Figure 7. Surface sensible heat flux (Wm^{-2}). For color-coding see Fig. 3.

3. PRELIMINARY RESULTS

Figure 4 shows the diagnosed boundary layer heights (BLH) for all the SCM simulations defined as in Cuxart et al. (2006), i.e. the height to where the turbulent momentum flux has decreased to 0.95% of its surface value divided by 0.95. This might not be a good way of defining the BLH at daytime, but it illustrates the large variation that is found between the models. No observations are included in the figure.

Even though the surface temperature is given in the case setup, the SCM give quite different 2-m temperatures (Figure 5). The intermodel spread, during both day and night, is approximately 2 degrees. The surface stress, represented by the surface friction velocity, is shown in Figure 6 also varies quite a low between the models. However, the difference between the models and the observations are more substantial, especially during nighttime. The second night, the models all give a much larger friction velocity than the observations show; this could partly be due to the somewhat to large prescribed geostrophic wind (see Figure 1).

Figure 7 shows the sensible heat flux that dominates clearly over the latent heat flux (not shown) in this dry environment. The models overestimate the downward heat flux for both nights compared with the observations. Some models do get a similar heat flux as the observations in the afternoon, but all lag behind in the morning. The magnitude of the flux is overestimated during the second night as well.

The 10m-wind speed is presented in Figure 8. As in the first GABLS experiment (Cuxart et al. 2006), many models have a too high wind speed during night. However, the most remarkable deviation from the observations is found during the morning hours. Almost all models have a decrease in the wind speed during the morning hours while the observations show a very sudden increase in the wind as it becomes convective. The modeled daytime wind speeds are generally for low during the daytime.

The 10-m wind is examined further in Figure 9 for October 23, where the diurnal amplitude is presented, i.e. each models mean wind is subtracted. The same procedure is applied for the observations both for the actual day and as a mean value for the entire month.

As can be seen in the figure, October 23 is a representative day for CASES 99. All models have a too small diurnal cycle around a, for most models, too high mean wind speed. Note that the color-coding in Figure 9 is different, here, the models are grouped according to their turbulence closure but there is no obvious difference between them.

The vertical structure in the modeled wind speed and temperature, including results from the three-dimensional COAMPS simulation as well as the observations are shown in Figure 10. Note the very different structure in the wind even though the simulated temperature structure is rather similar.

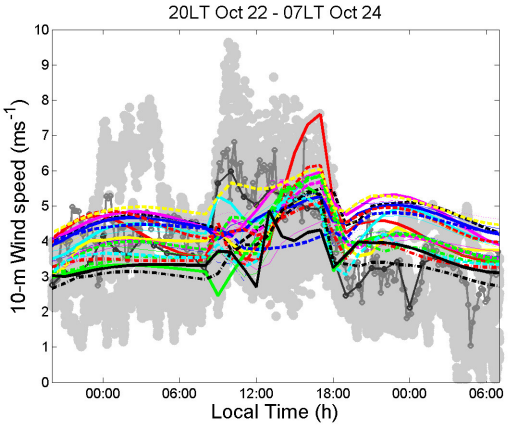

Figure 8. 10-m wind speed (ms^{-1}). For color-coding see Fig. 3. The gray lines are tower observations from the main site, the gray dots represent an area of approximately 50x50km^2 around the main tower.

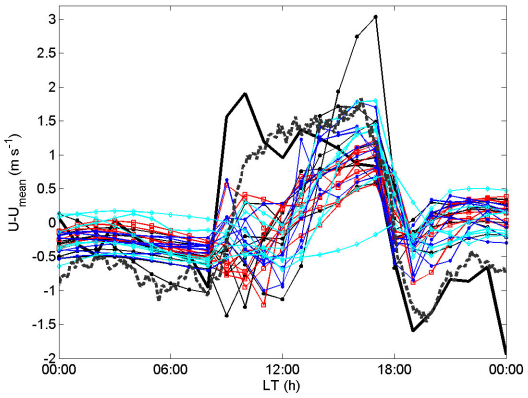

Figure 9. Diurnal amplitude of the10-m wind speed (ms^{-1}). The black solid line is the averaged amplitude for the entire month of October, the gray dashed line is for October 23. SCM results, 1st order closures (black and red) and turbulence models (blue and cyan).

3. CONCLUSION

The first conclusion from the second GABLS experiment, based on CASES99 data, is that the models produce very different results in all parameters and that they all differ substantially from the observations.

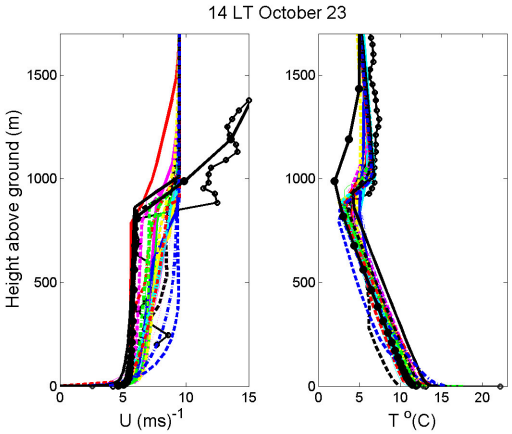

Figure 10. Wind speed (ms^{-1}) and temperature (^oC) for the lowest 1700m at 14LT October 23, 1999. Results from the three-dimensional COAMPS simulation (black line with filled circles) as well as sounding and tower data are included in the figure. For color-coding see Fig. 3.

The models range from first order closures with vertical resolutions used in numerical weather prediction models to higher order closure models with very fine mesh. The models were all forced with a prescribed surface temperature, based on observations, and a constant geostrophic wind. The validity of the magnitude of the wind forcing is checked by diagnosing the wind in a three-dimensional simulation with COAMPS. This analysis show that the COAMPS geostrophic wind is changing with time over the study period but the averaged value is about the same as the models were forced by.

When comparing the models and the observations, the most significant difference is the underestimated diurnal cycle in the 10-m wind speed. The modeled wind speeds are generally to high during the stably stratified night and to low during the unstably stratified daytime conditions. The difference is most striking during the morning hours where most models give a decrease in the wind speed while the observations, both for the selected day and as an average for the entire month of October, has a very distinct increase in the low-level wind speed as soon as the change to convective conditions occur.

Acknowledgements

We are devoted to the participating modeling groups for the time they have devoted to make the simulations. Thorsten Mauritsen, Gert-Jan.Steeneveld and Michael Tjernström are acknowledged for their valuable input.

REFERENCES

Beare, R.J., MacVean, M.K., Holtslag, A.A.M., Cuxart, J., Esau, I., Golaz, J-C., Jimenez, M.A., Khairoutdinov, M., Kosovic, B., Lewellen, D., Lund, T.S., Lundquist, J.K., McCabe, A., Moene, A.F., Noh, Y., Raasch, S. and Sullivan, P.P: 2006: An inter-

comparison of Large-Eddy Simulations of the stable boundary layer. *Boundary-Layer Meteorology.* In press in a special GABLS volume.

Cuxart, J., A.A.M. Holtslag, R.J. Beare, E. Bazile, A. Beljaars, A. Cheng, L. Conangla, M. Ek, F. Freedman, R. Hamdi, A. Kerstein, H. Kitagawa, G. Lenderink, D. Lewellen, J. Mailhot, T. Mauritsen, V. Perov, G. Schayes, G-J. Steeneveld, G. Svensson, P. Taylor, W. Weng, S. Wunsch, and K-M. Xu, 2006: Single-column model intercomparison for a stably stratified atmospheric boundary layer. *Boundary-Layer Meteorology.* In press in a special GABLS volume.

Hodur, R. M.,1997: The Naval Research Laboratory's Coupled Ocean/Atmosphere Mesoscale Prediction System (COAMPS). *Mon. Wea. Rev.,* **125**, 1414-1430.

Holtslag, A.A.M.: 2003: GABLS initiates intercomparison for stable boundary layers, *GEWEX news* **13**, 7-8.

Holtslag, A.A.M., 2006: Special Issue for Boundary Layer Meteorology: GEWEX Atmospheric Boundary Layer Study (GABLS) on Stable Boundary Layers. *Boundary-Layer Meteorology.* In press in a special GABLS volume.

Poulos, G.S. and Coauthors, 2002: CASES-99: A comprehensive investigation of the stable nocturnal boundary layer. *Bull. Amer. Meteor. Soc.,* **83,** 555–581.

Steeneveld, G.J., B.J.H. van de Wiel and A.A.M. Holtslag, 2006: Modeling the Evolution of the Atmospheric Boundary Layer Coupled to the Land Surface for Three Contrasting Nights in CASES-99, *J. Atmos. Sci.*, **63**, 920-935.

Svensson, G. And A.A.M. Holtslag, 2006: Analysis of model results for the turning of the wind in the stable boundary layer. *Manuscript.*